

Raman Spectroscopic Measurement of a Vacuum-Deposited C₆₀ Thin Film

Toshio Konno¹, Lingling Ren², Erlon H. Martins Ferreira³, Guangzhe Piao⁴,
 José Manuel Juárez García⁵, Froy Martínez Suárez⁶, Sergio J. Jimenez-Sandoval⁶,
 Takatsugu Wakahara¹ and Kun'ichi Miyazawa^{1,*}

¹ National Institute for Materials Science, Japan

² National Institute of Metrology, China

³ National Institute of Metrology, Quality and Technology, Brazil

⁴ Qingdao University of Science and Technology, China

⁵ National Center of Metrology, Mexico

⁶ Centro de Investigación y Estudios Avanzados del Instituto Politecnico Nacional, Mexico

Measurement of Raman shifts of a C₆₀ thin film and the evaluation of their uncertainties were conducted. A C₆₀ thin film with a thickness of about 1.2 μm was fabricated on a SiO₂ substrate by vacuum deposition. Raman spectra of the C₆₀ thin film were obtained using the laser beam power density of 5.7×10³ mW mm⁻². The measured Raman shifts were corrected according to the calibration curve that was prepared using sulfur and naphthalene as the reference samples. Standard uncertainties were calculated and combined in order to determine the combined uncertainty and the expanded uncertainty. It was found that the increase of measurement time and measurement points for the calibration curve leads to the higher reliability.

Keywords: C₆₀, Fullerene, Thin film, Raman spectrometry, Uncertainty.

PACS numbers: 68.35.bp, 78.30. – j

1. INTRODUCTION

The model of C₆₀ was proposed by Osawa in 1970 [1]. In 1985, C₆₀ was experimentally discovered by Kroto et al. [1]. The structure of C₆₀ is a truncated icosahedron composed of 60 carbon atoms with a diameter of 0.71 nm [3]. Belonging to point group I_h, a C₆₀ molecule has 174 internal degrees of freedom and 46 distinct vibrational modes as follows [4-12].

$$\Gamma_{vib} = 2A_g + 3T_{1g} + 4T_{2g} + 6G_g + 8H_g + A_u + 4T_{1u} + 5T_{2u} + 6G_u + 7H_u.$$

The A_g modes and H_g modes are Raman active [13-14]. Raman spectrometry is a powerful tool to understand the molecular and vibrational structure of C₆₀. Table 1 summarizes the measured Raman shifts of C₆₀ taken from literature [15-19]. Though the Raman shift of A_g(2) mode has been used to know the bonding state of C₆₀ molecules, the values in Table 1 are widely varying. It is considered that the variation resulted from different measurement conditions including the intensity of laser beam exposure, the wavelength of excitation laser beam and the calibration of spectrometer.

Table 1 – Raman shifts of the A_g modes and H_g modes of C₆₀ reported in literature.

Raman mode	Raman shifts (cm ⁻¹)				
A _g (1)	493	496	495	493	492
A _g (2)	1469	1470	1468	1463	1458
H _g (1)	270	273	271	270	273
H _g (2)	431	437	432	-	431
H _g (3)	709	710	709	707	709
H _g (4)	773	774	770	-	774
H _g (5)	-	1099	1097	-	1099
H _g (6)	1248	1250	1250	-	1248
H _g (7)	1426	1428	1426	1424	1425
H _g (8)	1573	1575	1574	1565	1572
C ₆₀	Film	Film	Film	Film	Powder
Ref.	[15]	[16]	[17]	[18]	[19]

* MIYAZAWA.Kunichi@nims.go.jp

In this paper, we measured a vacuum-deposited C₆₀ thin film by Raman spectrometry using weak laser beam power densities in order to avoid polymerization of C₆₀. Measured Raman shifts were calibrated using reference samples and the uncertainty was evaluated by considering calibration etc. The experimental details and results are shown below.

2. EXPERIMENTAL

2.1 Preparation of C₆₀ Thin Film

A C₆₀ thin film was prepared by vacuum deposition. 16 mg of C₆₀ powder (MTR Ltd., 99.99%) was ground using an agate mortar and mounted on a molybdenum boat. The boat and a 1-square-cm SiO₂ substrate were set in a vacuum deposition equipment (SANVAC, RD-1300R). The distance between the boat and the SiO₂ substrate was set to be 5 cm. The boat was heated by applying a voltage of 25~33 V under a vacuum of 10⁻⁴~10⁻³ Pa, monitoring the film thickness by a quartz oscillator.

2.2 Raman Spectroscopy Measurement

A Raman spectrometer, JASCO NRS-3100 equipped with a green laser of 532 nm wavelength, was used.

A calibration curve for the Raman spectrometer was prepared, using sulfur (SIGMA-ALDRICH, 99.998%) and naphthalene (SIGMA-ALDRICH, ≥99%) as the reference samples, according to ASTM E1840-96 [20].

The power of direct laser beam on the sample was measured using a silicon photodetector (Kaise, KT-2010).

Neutral density filters OD1, OD2 and OD3 were used to reduce the direct laser beam power to 1/10, 1/100 and 1/1000, respectively.

2.3 Uncertainty Evaluation in the Raman Measurement of C₆₀ Thin Film

According to the guides [21-24], the following four standard uncertainties are considered and combined to obtain the overall uncertainty, standard uncertainty of the mean of Raman shifts (u_{mea}), standard uncertainty of the calibration curve for the Raman spectrometer (u_{cal}), standard uncertainty of the Raman shifts of reference samples (u_{ref}), and standard uncertainty of the peak fitting (u_{fit}) of Raman profiles.

3. RESULTS AND DISCUSSION

3.1 Power Density of the Direct Laser Beam

The laser beam power density “ P [mW/mm²]” on a sample is defined by the following equation.

P = laser beam power [mW] / laser beam exposure area on the sample [mm²] (1), where, the laser beam exposure area on the sample = $\pi \times (\text{laser beam diameter} / 2)^2$, (2) and, the laser beam diameter on the sample = $1.22 \times \text{laser wavelength} / \text{objective numerical aperture}$ [25] (3).

Since an objective lens with an objective numerical aperture of 0.95 was used, the laser beam diameter on sample is calculated to be 0.68 μm from (3).

The power of direct laser beam on samples was measured to be 2.07 mW. Hence, using the above equations (1), (2) and (3), the power density of the direct laser beam on sample is calculated to be 5.7×10^6 mW / mm².

3.2 Preparation of the Calibration Curve using Reference Samples

The reference samples (sulfur and naphthalene) were measured with a laser beam power density of 5.7×10^5 mW / mm². Obtained Raman spectra are shown in Fig. 1. The referred values in literature [20] and the measured values of Raman shifts are shown in Table 2, and fitted by the linear least squares method to prepare the calibration curve shown in Fig. 2.

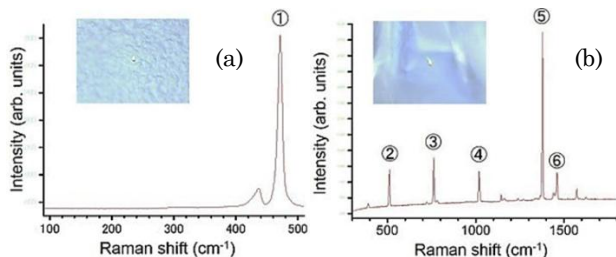


Fig. 1 – Raman spectra of (a) sulfur and (b) naphthalene measured by NRS-3100. Peak 1 ~ corresponds to the 1 ~ 6 points in Figure 2 and $i = 1 \sim 6$ in Table 2.

Table 2– Referred values (x_i) and measured values (y_i) of Raman shifts of sulfur and naphthalene. (i : sulfur and naphthalene band number.)

i	1	2	3	4	5	6
x_i cm ⁻¹	473.2	523.8	763.8	1021.6	1382.2	1464.5
y_i cm ⁻¹	471.4	510.9	761.6	1019.1	1378.2	1460.5

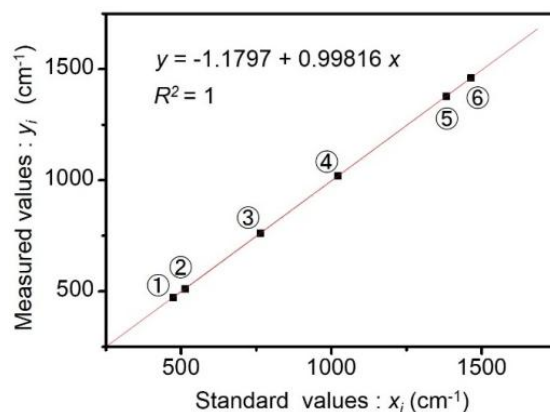


Fig. 2 – Calibration curve fitted by the linear least squares method. 1 ~ 6 corresponds to 1 ~ 6 in Figure 1 and $i = 1 \sim 6$ in Table 2

3.3 Raman Spectra of the Vacuum-Deposited C₆₀ Thin Film

As shown in Fig. 3, Raman spectra of the C₆₀ thin film were obtained, with an exposure time of 120 s and a sampling interval of 0.1 cm⁻¹ at a relative humidity of 42 % and room temperature. The Raman spectra were taken with varying the laser beam power density.

The spectrum of Fig. 3 (a) shows the broad bands around the peaks of $H_g(7)$ and $H_g(8)$ modes due to the damage caused by the high power density of 5.7×10^5 mW/mm². Although Fig. 3 (b) shows the disappearance of the above broad bands at the lower power density of 5.7×10^4 mW/mm², a shoulder peak of $A_g(2)$ is observed, showing the photopolymerization of C₆₀. However, Fig. 3 (c) shows no indication of polymerization of C₆₀. Hence, the measurement at the power density of 5.7×10^3 mW/mm² was conducted 5 times, changing the measurement place of the C₆₀ thin film.

The obtained spectra were corrected using the calibration curve (Fig. 2).

After the calibration, the Raman bands were fitted by Lorentzian functions using a software “Origin 9.1J (OriginLab Co., Northampton, MA, USA)” to determine the Raman shifts. The Raman shifts of the C₆₀ thin film are shown as X_j : the mean value of 5 measurements for each Raman mode (Table 3).

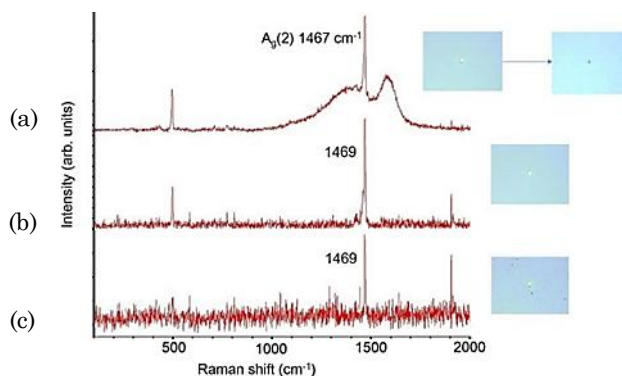


Fig. 3 – Raman spectra of the C₆₀ thin film taken with the laser beam power densities of (a) 5.7×10^5 mW/mm², (b) 5.7×10^4 mW/mm² and (c) 5.7×10^3 mW/mm².

Table 3 – Measured values and mean values of Raman shifts of the C₆₀ thin film after calibration.

<i>j</i> : C ₆₀ band number	1	2	3	4	5	6	7
Raman mode	<i>H_g(2)</i>	<i>A_g(1)</i>	<i>H_g(3)</i>	<i>H_g(4)</i>	<i>H_g(7)</i>	<i>A_g(2)</i>	<i>H_g(8)</i>
1 st measured cm ⁻¹	430.16	496.07	711.38	772.42	1423.91	1468.92	1575.01
2 nd cm ⁻¹	430.14	496.48	711.33	772.43	1424.66	1468.97	1574.79
3 rd cm ⁻¹	430.17	496.32	711.41	772.44	1424.55	1469.16	1575.19
4 th cm ⁻¹	430.17	496.02	711.35	772.44	1424.46	1468.70	1575.13
5 th cm ⁻¹	430.12	496.24	711.35	772.46	1424.55	1469.21	1575.09
Mean cm ⁻¹	430.15	496.23	711.36	772.44	1424.42	1468.99	1575.04

Table 4 – Standard uncertainty of the mean of Raman shifts of the C₆₀ thin film for each C₆₀ Raman mode.

<i>j</i>	1	2	3	4	5	6	7
Standard deviation cm ⁻¹	0.02	0.19	0.03	0.01	0.30	0.20	0.16
$(u_{mea})_j$ cm ⁻¹	0.01	0.08	0.01	0.01	0.13	0.09	0.07

Table 5 – Standard uncertainty of linear least squares calibration for each C₆₀ Raman mode.

Expression of $(u_{cal})_j$	$0.553 \sqrt{\frac{1}{5} + \frac{1}{6} + \frac{(Y_j - 933.62)^2}{904484}}$						
<i>j</i>	1	2	3	4	5	6	7
<i>Y_j</i> cm ⁻¹	428.18	494.13	708.87	769.84	1420.62	1465.11	1570.97
$(u_{cal})_j$ cm ⁻¹	0.45	0.42	0.36	0.35	0.44	0.46	0.50

Table 6 – Standard uncertainty of Raman shifts of reference samples.

<i>i</i>	1	2	3	4	5	6
Standard deviation cm ⁻¹ [20]	0.49	0.31	0.49	0.34	0.31	0.29
$(u_{ref})_i$ cm ⁻¹	0.19	0.12	0.19	0.13	0.12	0.11
u_{ref} cm ⁻¹	0.14					

Table 7 – Standard uncertainty of peak fitting of Raman profiles for each C₆₀ Raman mode.

<i>j</i>	1	2	3	4	5	6	7
u_{fit} for the 1 st profile cm ⁻¹	0.04	0.10	0.03	0.02	0.04	0.06	0.05
u_{fit} for the 2 nd cm ⁻¹	0.04	0.10	0.04	0.02	0.03	0.06	0.07
u_{fit} for the 3 rd cm ⁻¹	0.04	0.09	0.04	0.02	0.03	0.04	0.08
u_{fit} for the 4 th cm ⁻¹	0.04	0.11	0.04	0.02	0.03	0.05	0.08
u_{fit} for the 5 th cm ⁻¹	0.04	0.09	0.03	0.02	0.04	0.04	0.08
u_{fit} cm ⁻¹	0.04	0.11	0.04	0.02	0.04	0.06	0.08

3.4 Evaluation of Uncertainties

3.4.1 Standard uncertainty of the mean of Raman shifts (u_{mea})

The standard uncertainty of the mean u_{mea} is defined as follows.

$$u_{mea} = (\text{Standard deviation in measured Raman shifts of the C}_{60} \text{ thin film}) / \sqrt{m}, \quad (m : \text{number of measurement times to determine } X_j) \quad (4)$$

In this paper, $m = 5$.

u_{mea} of each Raman band, $(u_{mea})_j$, is shown in Table 4.

3.4.2 Uncertainty of the calibration curve for the Raman spectrometer (u_{cal})

The second is the standard uncertainty u_{cal} from linear least squares calibration. The inverse estimation using linear least squares calibration curve includes some uncertainties as shown in the following equations [24].

$$(u_{cal})_j = \frac{s}{b} \sqrt{\frac{1}{m} + \frac{1}{n} + \frac{(Y_j - \bar{y})^2}{b^2 \sum_{i=1}^n (x_i - \bar{x})^2}} \quad (5)$$

$$S = \sqrt{\frac{\sum_{i=1}^n \{y_i - (a + bx_i)\}^2}{n-2}} \quad (6)$$

Where a and b are the intercept and slope in the calibration curve, n is the number of measurement points for the calibration curve, Y_j is the mean value of 5 measurements for each C₆₀ Raman mode before calibration, \bar{x} is the mean of x_i and \bar{y} is the mean of y_i . In this paper, $a = -1.1797$, $b = 0.99816$, $m = 6$, $n = 5$, x_i and y_i are the values in table 2, $\bar{x} = 936.5$ and $\bar{y} = 933.6$. u_{cal} of each Raman mode, $(u_{cal})_j$, was calculated to be shown in Table 5 for respective Y_j .

3.4.3 Uncertainty of the Raman shifts of reference samples (u_{ref})

The standard uncertainty u_{ref} from the Raman shifts of sulfur and naphthalene was considered. u_{ref} for each sulfur and naphthalene Raman band $(u_{ref})_i$ is defined as follows.

Table 8 – Combined uncertainty and expanded uncertainty for each C₆₀ Raman mode.

j	1	2	3	4	5	6	7
$(u_{mea})_j$ cm ⁻¹	0.01	0.08	0.01	0.01	0.13	0.09	0.07
$(u_{cal})_j$ cm ⁻¹	0.45	0.42	0.36	0.35	0.44	0.46	0.50
u_{ref} cm ⁻¹	0.14						
$(u_{fit})_j$ cm ⁻¹	0.04	0.11	0.04	0.02	0.04	0.06	0.08
$(u_c)_j$ cm ⁻¹	0.47	0.47	0.39	0.38	0.48	0.49	0.53
U_j cm ⁻¹	0.94	0.93	0.78	0.75	0.96	0.98	1.06

Table 9 – Raman shifts and expanded uncertainty for each C₆₀ Raman mode.

Raman mode	$H_g(2)$	$A_g(1)$	$H_g(3)$	$H_g(4)$	$H_g(7)$	$A_g(2)$	$H_g(8)$
Raman shifts cm ⁻¹	430.15	496.23	711.36	772.44	1424.42	1468.99	1575.04
Expanded uncertainty cm ⁻¹	0.94	0.93	0.78	0.75	0.96	0.98	1.06

$(u_{ref})_i$ = (the standard deviation of the Raman shifts of sulfur and naphthalene) / \sqrt{l} (l : the number of laboratories to determine the Raman shifts). (7)

In this paper, $l = 7$ [20]. u_{ref} was evaluated by the following equation [23] and is shown in Table 6.

$$u_{ref} = \frac{\sum_{i=1}^n (u_{ref})_i}{n} \quad (8)$$

3.4.4 Uncertainty of peak fitting (u_{fit})

Standard uncertainty from peak fitting u_{fit} was calculated for each Raman profile using the standard error of x-coordinate of the vertex of fitted curve. u_{fit} for each Raman band of C₆₀, $(u_{fit})_j$, was evaluated as the maximum value in u_{fit} for the respective Raman profiles shown in Table 7.

3.4.5 Combined uncertainty and expanded uncertainty

Following the law of propagation of uncertainty, the combined standard uncertainty (u_c) is determined using the respective standard uncertainties.

$$u_c = \sqrt{(u_{mea})^2 + (u_{cal})^2 + (u_{ref})^2 + (u_{fit})^2} \quad (9)$$

REFERENCE

1. E. Osawa, *Kagaku* **25**, 854 (1970), (in Japanese).
2. H.W. Kroto, J.R. Heath, S.C. O'Brien, R.F. Curl, and R.E. Smalley, *Nature* **318**, 162 (1985).
3. W. Krätschmer, L.D. Lambt, K. Fostiropoulos, and D.R. Huffman, *Nature* **347**, 354 (1990).
4. Z.C. Wu, D.A. Jelski and T.F. George, *Chem. Phys. Lett.* **137**, 291 (1987).
5. R.E. Stanton and M.D. Newton, *J. Phys. Chem.* **92**, 2141 (1988).
6. F. Negri, G. Orlandi and F. Zerbetto, *Chem. Phys. Lett.* **144**, 31 (1988).
7. D.E. Weeks, and W.G. Harter, *J. Chem. Phys.* **90**, 4744 (1989).
8. J.L. Feldman, J.Q. Broughton, L.L. Boyer, D.E. Reich, and M.D. Kluge, *Phys. Rev. B* **46**, 731 (1992).
9. R.A. Jishi, R.M. Mirie, M.S. Dresselhaus, *Phys. Rev. B* **45**, 13685 (1992).
10. J. Kohanoff, W. Andreoni and M. Parrinello, *Phys. Rev. B* **46**, 4371 (1992).
11. X.Q. Wang, C.Z. Wang, and K.M. Ho, *Phys. Rev. B* **48**, 1884 (1993).
12. P. Giannozzi and S. Baroni, *J. Chem. Phys.* **100**, 8537 (1994).
13. J.C.R. Faulhaber, D.Y.K. Ko and P. R. Briddon, *Phys. Rev. B* **48**, 661 (1993).
14. K.P. Bohnen, R. Heid, K.M. Ho and C.T. Chan, *Phys. Rev. B* **51**, 5805 (1995).
15. A.M. Rao, P. Zhou, K.A. Wang, G.T. Hager, J.M. Holden, Y. Wang, W.T. Lee, X.X. Bi, P.C. Eklund, D.S. Cornett, M.A. Duncan, I.J. Amster, *Science* **259**, 955 (1993).
16. D.S. Bethune, G. Meijer, W.C. Tang, H.J. Rosen, W.G. Golden, H. Seki, C.A. Brown, M.S. Vries, *Chem. Phys. Lett.* **179**, 181 (1991).
17. K. Ikeda, and K. Uosaki, *J. Phys. Chem. A* **112**, 790

And it is necessary that u_c for each Raman band of C₆₀, $(u_c)_j$, is determined.

$$(u_c)_j = \sqrt{(u_{mea})_j^2 + (u_{cal})_j^2 + u_{ref}^2 + (u_{fit})_j^2} \quad (10)$$

At last, the expanded uncertainty (U) is decided for the higher reliability.

$$U = k u_c \quad (11)$$

$$U_j = k (u_c)_j \quad (12)$$

Where k is a coverage factor. In this paper, $k=2$. Table 8 shows all $(u_c)_j$ and U_j .

4. CONCLUSION

The Raman shifts and expanded uncertainty of respective C₆₀ Raman modes were determined using the vacuum-deposited C₆₀ thin film. The final results are shown in Table 9. The Raman shift of $A_g(2)$ was determined to be 1468.99 ± 0.98 cm⁻¹. As the most influential factor was u_{cal} , the increase of measurement time of specimen (m) and measurement points for the calibration curve (n) leads to the higher reliability.

- (2008).
18. E. Alvarez-Zauco, H. Sobral, E.V. Basiuk, J. M. Saniger-Blesa, M. Villagrán-Muniz, *Appl. Surf. Sci.* **248**, 243 (2005).
 19. X.H. Chen, X.J. Zhou and S. Roth, *Phys. Rev. B* **54**, 3971 (1996).
 20. The ASTM Committee on Standards. E1840-96, "Standard Guide for Raman Shift Standards for Spectrometer Calibration", 2007.
 21. The Joint Committee for Guides in Metrology (JCGM), "Guide to the Expression of Uncertainty in Measurement", 2008.
 22. Stephanie Bell, Measurement Good Practice Guide No. 11 (Issue 2), A Beginner's Guide to Uncertainty of Measurement, National Physical Laboratory, 2001.
 23. EURACHEM/CITAC Working Group, "Quantifying Uncertainty in Analytical Measurement", 2000.
 24. National Institute of Technology and Evaluation, "Japan Calibration Service System JCG200S21", 2011.
 25. F. Adar, S. Mamedov, and A. Whitely, *Microsc. Microanal.* **11**, 728 (2005).